Photo, Thermal, and Ultrasonic Degradation of EGDMA-Crosslinked Poly(acrylic acid-*co*-sodium acrylate-*co*-acrylamide) Superabsorbents

Neelesh Bharti Shukla, Giridhar Madras

Department of Chemical Engineering, Indian Institute of Science, Bangalore 560012, India

Received 21 April 2011; accepted 26 September 2011
DOI 10.1002/app.36289
Published online 26 December 2011 in Wiley Online Library (wileyonlinelibrary.com).

ABSTRACT: Superabsorbent polymers (SAPs) based on acrylic acid (AA), sodium acrylate (SA), and acrylamide (AM) were synthesized by inverse suspension polymerization using ethylene glycol dimethacrylate as the crosslinking agent. The equilibrium swelling capacities and the rates of swelling of SAPs varied with the AM content and followed first-order kinetics. The photodegradation of SAPs in their equilibrium swollen state was carried out by monitoring their swelling capacity and the residual weight fraction. The SAPs degraded in two stages, wherein the swelling capacity increased to a maximum and then subsequently decreased. Thermogravimetric analysis of the SAPs indicated that the copolymeric superabsorbents had intermediate thermal stability between the homopolymeric superabsorbents. The activation energies of SAPs with 0, 20, and 100 mol % AM content were determined by Kissinger method and were found to be 299, 248, and 147 kJ mol^{-1}, respectively. The ultrasonic degradation of the superabsorbents was carried out in their equilibrium swollen state, and the change in the viscosity with ultrasonication time was used to quantify the degradation. The ultrasonic degradation of AA/SA superabsorbent was also investigated at various ultrasound intensities. The degradation rate coefficients were found to increase with the intensity of ultrasound. The ultrasonic degradation of AA/SA/AM (20% AM) was also carried out, and degradation rate was found to be more than that of the AA/SA superabsorbent. J Appl Polym Sci 125: 630–639, 2012

Key words: acrylic acid; superabsorbent; hydrogel; degradation; photodegradation; ultrasound

INTRODUCTION

Superabsorbent polymers (SAPs) are water-insoluble three-dimensional crosslinked network structures of hydrophilic monomers. They have the ability to absorb water or aqueous solutions up to several hundred times of their own weight. Because of their extremely high liquid absorption and retention properties, they are most widely used in personal hygiene products such as diapers, sanitary napkins, and adult incontinence products[1] and constitute a large part of domestic waste. They find applications as controlled drug delivery devices[2] and contact lenses[3] in the biomedical field. They are also used for food packaging, water purification,[4–6] and improvement of water retention of soil.[7]

Some important characteristics of the SAPs are their equilibrium swelling capacity, swelling rate, reversible swelling/deswelling behavior depending on the surrounding medium, and ability to adsorb oppositely charged materials. Various SAPs have been synthesized by copolymerization of acrylic acid (AA) with acrylamide (AM),[7–9] *N*-isopropylacrylamide,[10] 2-(dimethylamino)ethyl methacrylate,[10] sodium allyl sulfonate,[11] and itaconic acid.[4] The effect of various parameters such as polymerization temperature, initiator concentration,[12] degree of neutralization of AA,[13,14] and concentration of the crosslinking agent[7,8,14] has also been studied. Different crosslinking agents such as *N*,*N*′-methylene bisacrylamide,[10,14] ethylene glycol dimethacrylate (EGDMA),[15,16] trimethylol propane triacrylic ester,[17,18] modified poly(ethylene glycol),[19] glyoxal bis(diallyl acetal),[20] divinyl sulfone,[21] glutaraldehyde, and divinylbenzene[22] have been used to impart crosslinks. The superabsorbents based on natural materials such as starch,[11] cellulose,[21] chitosan,[23,24] and gelatin[25] have also been developed.

The synthesis of various SAPs based on both natural and synthetic monomers is well established. Although there are many studies of enzymatic degradation of SAPs based on natural sources,[26,27] there is not much information available about the degradation of the SAPs based on synthetic monomers such as AA and AM. Li and Cui[28] have reported ultraviolet-induced degradation of AA- and AM-based superabsorbents by monitoring the weight at

Correspondence to: G. Madras (giridhar@chemeng.iisc.ernet.in).

Contract grant sponsor: Department of Science and Technology, India

the end of the degradation. The study does not provide much information about the kinetics of degradation, swelling/deswelling behavior, and the changes in the swelling capacity on degradation of the superabsorbents under investigation.

The ultrasonic degradation of the polymers is interesting because of its distinctive characteristics such as preferential scission at the mid-point of the chain,[29] higher rates of degradation of the higher molecular weight species, and existence of a limiting molecular weight below which degradation does not occur.[30] The ultrasonic degradation of the water-soluble polymers such as poly(ethylene oxide),[30] poly(acrylamide),[30] and poly(acrylic acid)[31] has been widely studied; however, there are no reports of the degradation of AA-based crosslinked SAPs.

In the current study, poly(acrylic acid-*co*-sodium acrylate-*co*-acrylamide) superabsorbents crosslinked with EGDMA have been prepared via inverse suspension polymerization technique. The AM content was varied from 0 to 100 mol %, and the synthesized SAPs had a wide range of equilibrium swelling capacity. The degradation of SAPs was carried out in their equilibrium swollen state by exposure to UV radiation and ultrasound and in the dry state by thermogravimetric analysis (TGA). To the best of our knowledge, photodegradation of the SAPs discussed here is the first study in which the degradation was monitored by measuring swelling capacity of the SAPs and correlating it with the residual weight fraction to understand the degradation process. Furthermore, this is the first study of the ultrasonic degradation of the SAPs in which the degradation of the swollen gel has been observed by the change in viscosity.

EXPERIMENTAL

Materials

AA and AM monomers were obtained from Merck (Mumbai, India) and S.D. Fine-Chem (Mumbai, India), respectively. EGDMA used as the crosslinking agent was procured from Aldrich. Sodium hydroxide and potassium persulfate (KPS) were purchased from S.D. Fine-Chem. Hydrochloric acid and methanol were procured form Merck. The surfactant Span-80 was obtained from Rolex Chemical Industries (Mumbai, India). Milli-Q deionized (DI) water was used for all the experiments.

Synthesis of the SAPs

The technique of inverse suspension polymerization was used for the synthesis of the SAPs.[16] The SAPs were synthesized in a four-necked round-bottomed flask equipped with a reflux condenser, an inlet for N_2, and a temperature sensor. The reactants were added from the fourth inlet. A heating mantle with a magnetic stirrer was used to carry out the polymerization.

The dispersed phase consisted of monomers AA, sodium acrylate (SA), and AM in appropriate molar ratios in DI water. SA was obtained by 75% neutralization of AA by NaOH solution. The initiator, KPS, 0.5 mol % of total monomers, was dissolved in the dispersed phase, and the dispersed phase was purged with N_2 for 15 min before being added dropwise to the continuous phase. The continuous phase contained toluene (90 mL), water-in-oil surfactant Span-80 (0.33 vol % of toluene), and the crosslinking agent EGDMA (0.5 mol % of total monomers). The dispersed phase was added dropwise to the continuous phase, and the polymerization was carried out for 2 h under N_2 bubbling at 80°C. After the polymerization, the unreacted monomers and water were removed by adding excess of methanol, and the polymer was dried for 72 h at 80°C in a hot air oven. Further details of the polymerization are given elsewhere.[32] Poly(acrylic acid-*co*-sodium acrylate-*co*-acrylamide) superabsorbents having 20, 40, 60, 80, and 100 mol % AM were named as AA/SA/AM-1, AA/SA/AM-2, AA/SA/AM-3, AA/SA/AM-4, and AM-1, respectively.

The swelling capacity of the SAPs increases with increasing crosslink density, reaches a maximum at an optimum crosslink density, and then decreases as the network becomes denser. Based on the literature,[8,9] an optimum crosslinking agent concentration of 0.5 mol % of total monomer was chosen.

Fourier transform infrared spectroscopy

Perkin Elmer Spectrum RX-I spectrometer was used to carry out the Fourier transform infrared spectroscopy (FTIR) of the SAPs. The spectra were recorded in transmission mode at a resolution of 4 cm^{-1} in the range of 4000 to 500 cm^{-1}. The FTIR spectra thus obtained are reported elsewhere.[32]

Determination of swelling capacity of the SAPs

The swelling capacity of the SAPs used in this study was determined gravimetrically. A known weight of the dry SAP was kept in a plastic basket and immersed in glass beakers containing 500 mL of DI water. The baskets were removed at different times, and the excess water was removed by wiping them with tissue papers. The swollen samples were weighed on a Sartorius BP121 S weighing balance and replaced in the respective beakers for further swelling. Six samples were taken for each experiment, and the reported data points represent the

averages of the six data points. The error was found to be less than ±2%.

Photodegradation of equilibrium swollen SAPs

Photodegradation setup

About 0.1 g of dry SAP was swollen to its equilibrium swelling capacity by immersing it in 500 mL of DI water for 10 h. As shown in Figure 1, the glass beakers containing equilibrium swollen polymers were kept concentrically around a 125-W high-pressure mercury vapor lamp (Philips, India), which was kept inside a jacketed quartz tube (3.4 cm i.d., 4 cm o.d., and 20 cm length). Each glass beaker containing swollen polymer was exposed to UV radiation for a certain period of time. The degradation of polymers was monitored by determining the swelling capacity and the residual weight. After exposure to the UV radiation, the swollen polymers were transferred to perforated cups made of aluminum foil. The swelling capacity was determined gravimetrically after draining out the excess water. The swollen polymers kept in aluminum foil cups were dried in hot air oven at 80°C for 72 h and then weighed to determine the residual weight of the dry polymer.

Determination of the intensity of UV radiation

Prior to the photodegradation of the SAPs, the intensity of the UV radiation emitted from the high-pressure mercury vapor lamp was measured by a UV light meter (UV-340, Lutron). The intensity was measured at the front of the beaker ($R_1 = 5.5$ cm), center of the beaker ($R_2 = 10.0$ cm), and at the backside of the beaker ($R_3 = 14.5$ cm; Fig. 1). The intensity of the UV radiation was also measured at $R_2 = 10.0$ cm with and without the beaker.

Thermal degradation of dry SAPs

Pyris TG/DTA system (Perkin Elmer, USA) was used to carry out the thermal degradation of dry SAPs. About 2.0 mg of dry SAP was subjected to thermal degradation in an inert atmosphere under the N_2 flow at 150 cm^3 min^{-1}. The samples were heated from 25 to 500°C at constant heating rates of 5, 10, 15, 20, 25, and 30°C min^{-1}.

Ultrasonic degradation of the SAPs

The ultrasonic degradation of the superabsorbents was carried out in their equilibrium swollen state. About 0.1 g of the SAP was swollen to its equilibrium swelling capacity in 100-mL beakers. Excess water was drained out and the swollen gel was subjected to the ultrasonic degradation for different times using a horn-type ultrasonic processor (Vibronics, Mumbai, India) at various intensities. For all the experiments, the horn was dipped to the middle of the swollen gel, and the beakers were placed in a thermostated water bath to maintain the temperature at 25°C. The ultrasonic degradation of the SAPs was monitored by measuring the changes in the viscosity. The viscosity measurements of the gel were carried out on an AR1000 Rheometer (TA Instruments, New Castle, DE), and the gel was sheared using a parallel-plate geometry (diameter = 4.0 cm, gap thickness = 0.4 mm) at a constant shear stress of 10 Pa. To study the effect of intensity on the ultrasonic degradation of swollen hydrogels, homopolymeric AA/SA-1 was exposed to ultrasound of different intensities. AA/SA/AM-1 copolymeric superabsorbent, with 20% AM content, was also subjected to ultrasonic degradation to investigate the effect of AM content on the degradation.

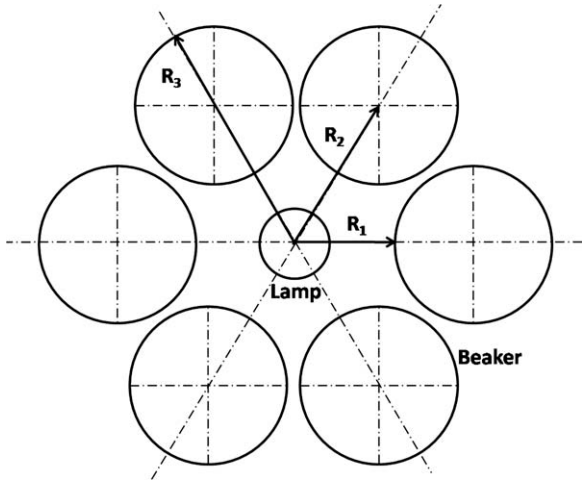

Figure 1 The schematic of photodegradation setup.

RESULTS AND DISCUSSION

Equilibrium swelling capacity and swelling kinetics of the SAPs

The superabsorbent characteristics of the crosslinked polymers based on partially neutralized AA result from the electrostatic repulsion between the negatively charged carboxyl groups of the polymer backbone, which tend to expand the three-dimensional network.[33] Because of the Donnan membrane equilibria between the ionic polymer and its surrounding water, the swollen polymer acts as its own membrane and prevents the mobile charges from diffusing into the surroundings. The attracting power of fixed charges always maintains higher concentration of mobile ions inside the swollen polymer than that in the surroundings. The osmotic pressure inside the polymer exceeds that of the swelling medium and results in the expansion of the network by the intake of a

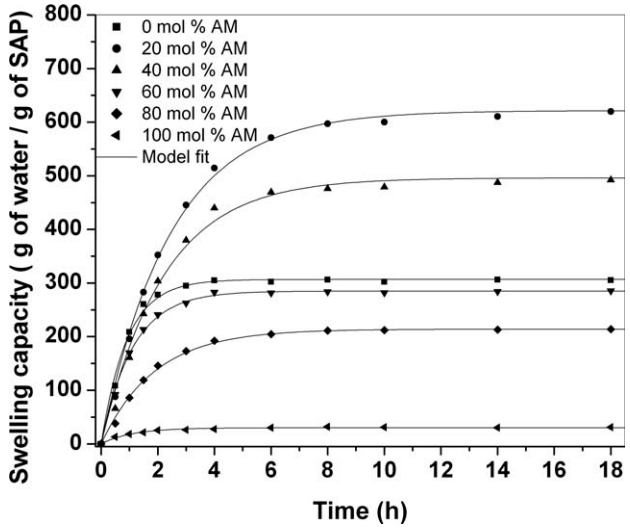

Figure 2 Variation in the swelling capacity of the SAPs with time.

large quantity of water. On swelling, the polymer chains assume elongated configurations and an elastic retractive force develops opposing the swelling process. The equilibrium swelling capacity is achieved when these two opposing forces balance each other.

The swelling capacity (S) of the SAPs (g of water/g of the SAP) is given as follows:

$$S = \frac{W_s - W_d}{W_d} \quad (1)$$

where W_d and W_s are the weights of the dry and swollen SAP, respectively. Figure 2 exhibits the variation of the experimental swelling capacity of various SAPs with time and the first-order model fit. All the SAPs in this study followed the first-order swelling kinetics. The first-order swelling kinetics has been previously reported for SAPs of AM with anionic monomers,[7] carboxymethyl cellulose-*g*-poly (acrylamide-*co*-2-acrylamido-2-methylpropan sulfonic acid),[34] and anionic and cationic starch-based superabsorbents.[35] The same model, eq. (3), is used here for the swelling kinetics.

$$\frac{dS}{dt} = k_s(S_{eq} - S) \quad (2)$$

where k_s is the swelling rate constant, and S and S_{eq} are the swelling capacities at any time t and at equilibrium, respectively. At $t = 0$, $S = S_0 = 0$, and as $t \rightarrow \infty$, $S = S_{eq}$

$$S = S_{eq}[1 - \exp(-k_s t)] \quad (3)$$

It can be noticed from Figure 2 that water is absorbed at a faster rate in the early stages of degradation and then the rate of water absorption reduces slowly until the SAPs achieve their equilibrium swelling capacity. According to Flory-Rehner theory,[33] mixing, elastic, and ionic contributions dictate the swelling characteristics of ionic networks. Initially, the osmotic pressure difference between the polymer network and swelling medium is very high, and thus, water diffuses rapidly into the network. With the absorption of water, the osmotic pressure difference reduces, elastic retractive forces overcome the driving force for absorption, and thus, the rate of water uptake slows down. This phenomenon of change of rate of absorption with the swelling is very well described by the first-order swelling kinetics [eq. (3)] and is consistent with other studies.[7,34,35] Equation (3) describing the first-order kinetics of the swelling of the SAPs also resembles the Voigt model $\varepsilon(t) = (\sigma_0/E)[1 - \exp\{(t_0 - t)/\tau_0\}]$ used by Omidian et al.,[36] where $\varepsilon(t)$ is strain at time t, σ_0 is applied stress, E is elastic modulus, and τ_0 is retardation time. The characteristic constants σ_0/E and τ_0 are equivalent to the equilibrium swelling (S_{eq}) and inverse of swelling rate constant (k_s).

The equilibrium swelling capacities and swelling rate constants obtained from the first-order swelling model are given in Table I. AA/SA/AM-1 (20 mol % AM) exhibits the highest equilibrium swelling capacity, whereas AM-1 (100 mol % AM) has the lowest swelling capacity. The addition of 20 and 40 mol % AM to AA/SA results in the increase of the swelling capacity of the copolymeric hydrogels. Similar results have been obtained in the investigation of AA/AM SAPs crosslinked with *N*,*N*′-methylene bisacrylamide, in which the SAP with 15 wt % AM content showed the highest swelling capacity.[9] Among the copolymeric superabsorbents, the number of the anionic repeat units decreases with increase in the mole percent of AM resulting in the lowering of the equilibrium swelling capacity. Among the SAPs, AA/SA-1 shows the highest rate of swelling because of the highest number of anionic units resulting in higher osmotic pressure difference when compared with other SAPs.

The homopolymeric AA/SA-1 superabsorbent has a very high density of anionic repeat units. The

TABLE I
Composition and Kinetic Parameters for the Swelling of SAPs

SAP	AA/SA (mol %)	AM (mol %)	S_{eq} (g of water/g of SAP)	k_s (h^{-1})
AA/SA-1	100	0	306.80	1.098
AA/SA/AM-1	80	20	621.69	0.408
AA/SA/AM-2	60	40	496.11	0.454
AA/SA/AM-3	40	60	285.03	0.892
AA/SA/AM-4	20	80	215.03	0.530
AM-1	0	100	30.08	0.902

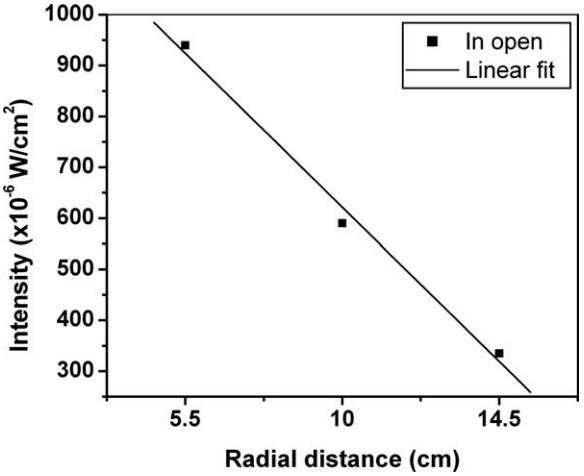

Figure 3 Variation in the intensity of UV radiation with the radial distance.

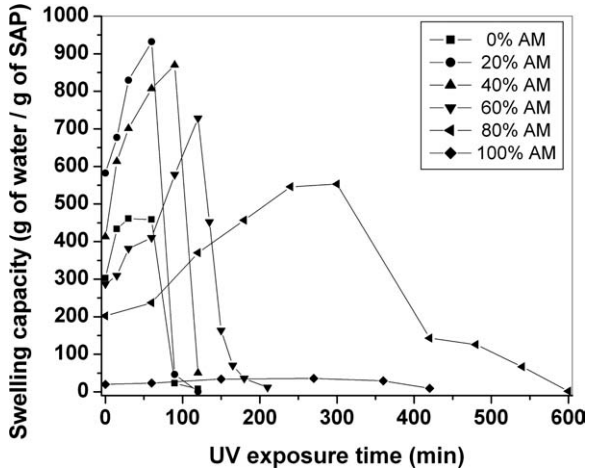

Figure 4 Variation of swelling capacities of the SAPs with the UV exposure time.

presence of ionic repeat units is necessary for the superabsorbent nature of the polymers, but an excess of them results in a network, where effective expansion is reduced due to the action of two forces acting in opposite direction. By copolymerizing AA/SA with AM, nonionic repeat units are introduced into the network, which act as spacer between the anionic units. Although, the osmotic pressure decreases due to reduction in ionic repeat units but, the increased separation allows more expansion of the network resulting in higher swelling capacity. Thus, SAPs with 20 and 40 mol % AM show higher swelling capacity than that with 0 mol % AM. But, beyond a certain extent of nonionic repeat units, the osmotic pressure decreases to a great extent causing lowering of swelling capacity. Thus, SAPs with 60 and 80 mol % AM have lower swelling capacity than AA/SA-1 (0 mol % AM).

The rate of swelling is affected by the number of anionic repeat units and also by the molecular weight between the crosslinks (M_c). The variation in M_c of various SAPs, along with the changing ionic content, could give rise to the variation in rates of swelling, and thus, the rate of swelling does not follow a trend similar to that followed by the equilibrium swelling capacity.

Photodegradation of SAPs

The intensity of the UV radiation was determined prior to the photodegradation experiments and was found to decrease with increasing distance along the radial direction. Figure 3 shows the variation in the intensity of UV radiation with the distance from the center of the lamp. As all the samples were positioned around the lamp at the same radial distance, they were irradiated with the same intensity of UV radiation. The intensity at the center of the glass beaker at $R_2 = 10$ cm was found to be 576 μW cm^{-2} and was only slightly lesser than that, 590 μW cm^{-2}, at the same distance when measured without the beaker. The UV–visible spectra of the SAPs indicated that the SAPs do not absorb light in visible region, and thus, the photodegradation results from the interaction of the UV radiation with the SAPs.

The photodegradation of the SAPs was carried out in their equilibrium swollen state. The photodegradation was monitored by monitoring the swelling capacity and the residual weight fraction of the polymer (Figs. 4 and 5). All the SAPs exhibited similar behavior when exposed to UV radiation. The UV exposure time of the SAPs can be divided into two regions (Fig. 6). In the first region of duration t_1, the swelling capacity of the SAPs increased and reached to a maximum value, S_{max}. In the second region of duration t_2, the swelling capacity as well as residual weight fraction dropped drastically. The swelling

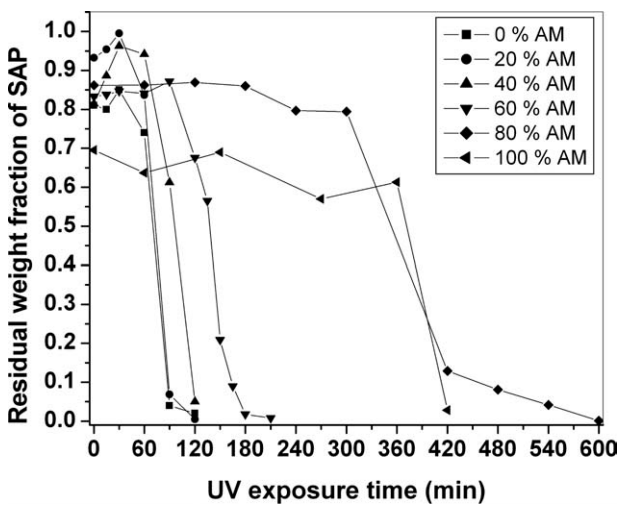

Figure 5 Variation of residual weight fraction of the SAPs with the UV exposure time.

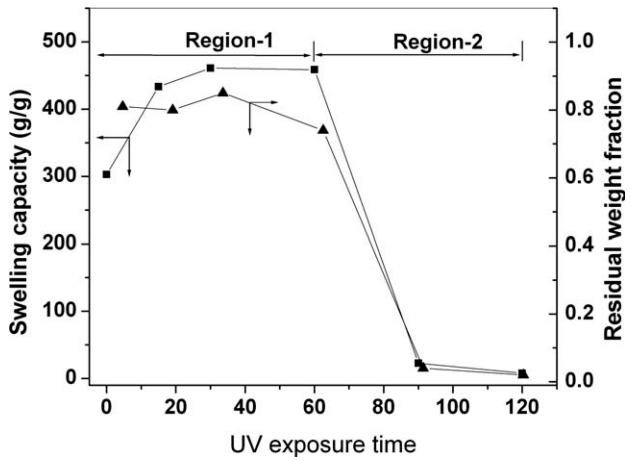

Figure 6 Variation of swelling capacity and residual weight fraction of AA/SA-1 with the UV exposure time.

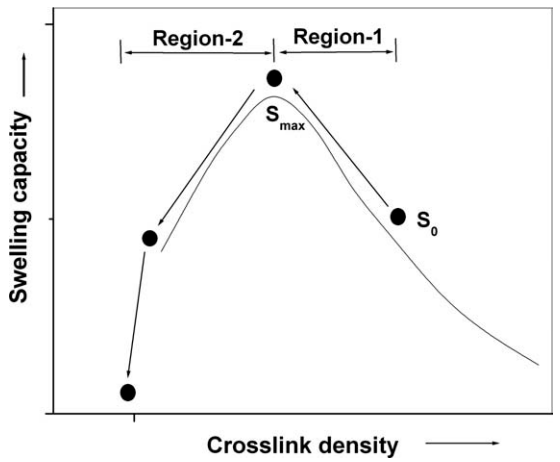

Figure 7 Schematic of variation in swelling capacity with crosslink density during the UV degradation of the SAPs.

capacity of the SAPs depends on the crosslink density and thus on the crosslinking agent concentration. With the increment in crosslink density, the swelling capacity increases, reaches a maximum at an optimum crosslink density, and then decreases as the network becomes denser.[7–9,14,17,19]

In the current study, on exposure to the UV radiation, the swelling capacity increased first, achieved a maximum value, and then decreased. Thus, the initial SAPs were highly crosslinked, and on exposure to UV radiation, their crosslink density decreased and reached an optimum value corresponding to maximum swelling capacity. Further exposure resulted in the degradation of the network and in the lowering of swelling capacity of the gel (Fig. 7). The observation of residual weight fraction of the SAPs during the photodegradation also supports the above-mentioned phenomena. In Figure 6 for AA/SA-1, it can be observed that the residual weight fraction remains nearly constant during the first region of the degradation, confirming that only the earlier dense network becomes sparse in this region. The sudden drop in the residual weight fraction in the second region is due to the degradation of the insoluble networked structure resulting in the formation of water-soluble polymers. There was no bubble formation observed during the degradation, indicating the absence of any volatile products on the degradation. The temperature of the samples was monitored during the degradation, and it was found that UV radiation did not cause any significant increase in temperature. Thus, the deswelling was not due to the increase in temperature.

Table II lists the initial swelling capacity (S_0), maximum swelling capacity (S_{max}), and the time t_1 and t_2 for the two degradation regions. AA/SA-1 and AA/SA/AM-1 are equally resistant to UV radiation. As the AM content increased from 20 to 80%, the time scale of the first region increased, indicating improvement in the UV resistance of the SAPs. The improvement in the SAPs UV resistance with increasing AM content conforms with the study of photocatalytic degradation of poly(acrylamide-*co*-acrylic acid).[37] There is 1.52–2.73 times increment in the swelling capacity of the SAPs in the first region, indicating that the crosslinking agent concentration used is more than the optimum resulting in a dense network and still higher swelling capacities can be obtained by lower crosslinking agent concentrations. Thus, the photodegradation of SAPs can be qualitatively used to characterize the crosslink density of SAPs.

TABLE II
Change in Swelling Capacities and the Time Scales of the Two Photodegradation Stages

SAP	S_0 (g of water/ g of SAP)	S_{max} (g of water/ g of SAP)	S_{max}/S_0	t_1 (min)	t_2 (min)
AA/SA-1 (0% AM)	303	460	1.52	60	60
AA/SA/AM-1 (20% AM)	582	932	1.60	60	60
AA/SA/AM-2 (40% AM)	413	870	2.11	90	30
AA/SA/AM-3 (60% AM)	287	728	2.54	120	90
AA/SA/AM-4 (80% AM)	202	552	2.73	300	300
AM-1 (100% AM)	20	36	1.8	270	150

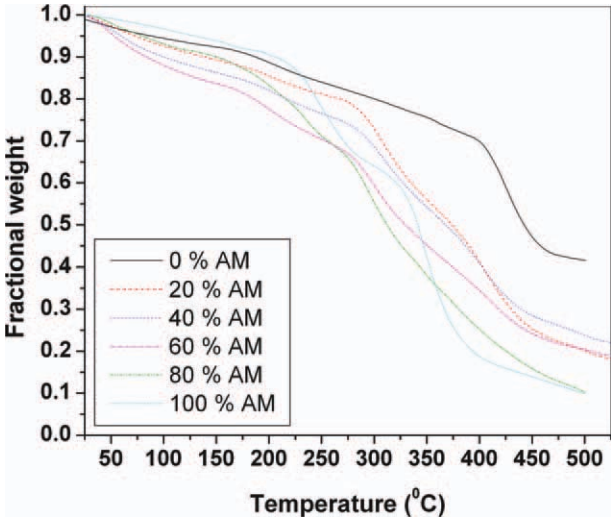

Figure 8 Thermogravimetric analysis curves of SAPs at a heating rate of 5°C/min. [Color figure can be viewed in the online issue, which is available at wileyonlinelibrary.com.]

Thermal degradation of SAPs

Figure 8 shows the weight loss profiles of various SAPs during the TGA at a heating rate of 5°C min^{-1}. Differential thermogravimetric (DTG) analysis plots (Fig. 9) differentiate between the various degradation regions of the SAPs. Homopolymeric superabsorbents AA/SA-1 and AM-1 decompose in two stages, and the copolymeric superabsorbent AA/SA/AM-1 undergoes degradation in three stages. Similar pathways of degradation have been previously reported for the poly(acrylic acid-*co*-sodium acrylate), poly(acrylamide), and poly(acrylic acid-*co*-sodium acrylate-*co*-acrylamide).[38] In the first stage (160–393°C) of AA/SA-1, the removal of moisture and decarboxylation overlap. The decomposition of polymer backbone takes place in the second stage (393–475°C) with the maxima at 424°C. AM-1

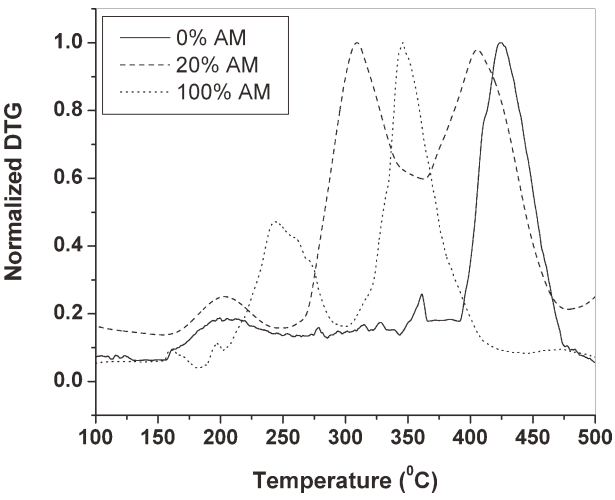

Figure 9 Normalized DTG plots of AA/SA-1, AA/SA/AM-1, and AM-1 at a heating rate of 5°C/min.

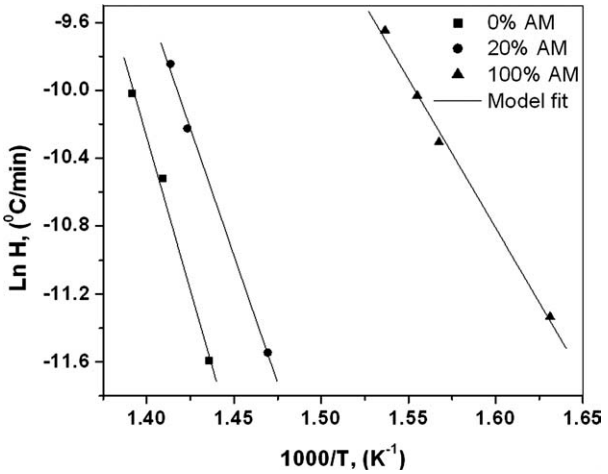

Figure 10 Kissinger plots of AA/SA-1, AA/SA/AM-1, and AM-1.

also decomposes in two stages: in the first stage (200–300°C), imidization of amide groups takes place, whereas in the second stage (300–450°C), the polymer backbone cleaves. AA/SA/AM-1 undergoes degradation in three stages. In the first region (160–250°C), removal of water and imidization occurs. In the second region (250–363°C), decarboxylation of the AA/SA units takes place. In the final stage (363–475°C), the copolymer chains break.

The activation energies were determined using thermograms at different heating rates by the Kissinger's method. The activation energies were calculated from the slope of plot of $\ln(\beta/T_m^2)$ vs $1/T_m$ using following equation:

$$\frac{d[\ln(\beta/T_m^2)]}{d[1/T_m]} = -\frac{E}{R} \quad (4)$$

β is heating rate, T_m is the temperature corresponding to maximum rate of weight loss, E is the activation energy, and R denotes universal gas constant. The Kissinger plots of AA/SA-1, AA/SA/AM-1, and AM-1 are shown in Figure 10. The estimated activation energies, using eq. (4), for AA/SA-1, AA/SA/AM-1, and AM-1 are 299, 248, and 147 kJ mol^{-1}, respectively.

Temperatures of SAPs during TGA at various conversions have been plotted in Figure 11. The numbers 0.1–0.9 in Figure 11 refer to the extent of thermal degradation of the SAPs. Figure 11 has only two data points for 0.9, as only the SAPs with 80 and 100 mol % AM content underwent more than 90% degradation. Because of the higher moisture content, AA/SA-1 is less stable than AM-1 at low conversions. After the initial loss of moisture for the same conversion, the temperature is always higher for AA/SA-1 than AM-1, indicating higher thermal stability of AA/SA-1 over AM-1. The thermal stability of AA/SA/AM-1 copolymeric superabsorbent is

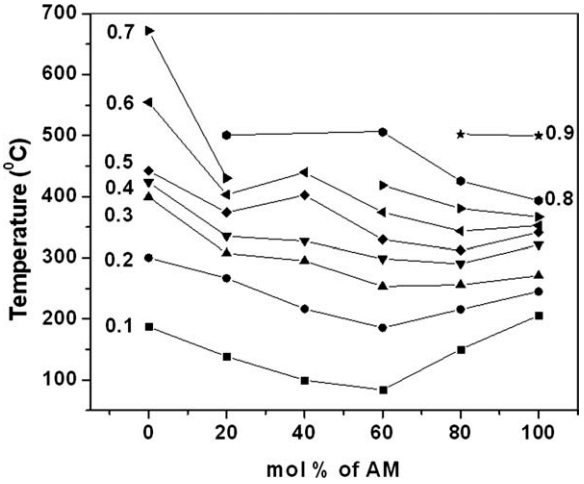

Figure 11 Temperatures of the SAPs during thermogravimetric analysis at various conversions. The numbers refer to the extent of thermal degradation.

lower than that of AA/SA-1, but higher than that of AM-1. The thermal behavior of the copolymeric superabsorbent is expected to be a hybrid of the parent homopolymeric superabsorbents, and these results are in accordance with the thermal degradation study of non-crosslinked poly(acrylamide) and poly(acrylamide-*co*-sodium acrylate).[38]

Ultrasonic degradation of the SAPs

Because of the insoluble nature of the crosslinked SAPs, the determination of the average molecular weights is not possible. Therefore, the viscosity of the equilibrium swollen gel can be used as an alternative parameter to quantify the degradation. The following rate equation, first order in viscosity, can be assumed to describe the degradation of the gels:

$$-\frac{d\mu}{dt} = k_{US}(\mu).\mu \tag{5}$$

where μ is the viscosity of the swollen gel at time t, and $k_{US}(\mu)$ is the ultrasonic degradation rate coefficient. $k_{US}(\mu)$ is assumed to be a linear function of viscosity, that is, $k_{US}(\mu) = \kappa_{US}(\mu - \mu_{lim})$. Similar dependence of the ultrasonic degradation rate coefficient on the MW has been previously reported.[30,31] The higher molecular weight species undergo degradation at a faster rate than those of lower molecular weights, and no degradation occurs below a limiting molecular weight.[30] This relationship ensures that the rate coefficient becomes zero when viscosity reaches the limiting viscosity (μ_{lim}) and no further degradation of the gel takes place. Thus,

$$-\frac{d\mu}{dt} = \kappa_{US}(\mu - \mu_{lim})\mu \tag{6}$$

which is second order in viscosity. Solving this with initial condition $\mu = \mu_0$ at $t = 0$ results in

$$\ln\left[\frac{\mu}{\mu_0}\frac{(\mu_0-\mu_{lim})}{(\mu-\mu_{lim})}\right] = \kappa_{US}\mu_{lim}t \tag{7}$$

$$\ln Y = \kappa_{US}\mu_{lim}t \tag{8a}$$

$$Y = \frac{\mu}{\mu_0}\frac{(\mu_0-\mu_{lim})}{(\mu-\mu_{lim})} \tag{8b}$$

The above-mentioned model can be successfully applied for the ultrasonic degradation of the SAPs, as the very high swelling capacities result in the polymer solutions having concentrations similar to those used for the ultrasonic degradation of soluble polymers.

The ultrasonic degradation of the polymers takes place due to the cavitation, growth, and rapid collapse of microbubbles. During the collapse of these microbubbles, intense shear fields are generated and the polymer chains in the proximity of the collapsing cavity move faster than those away from it. The relative motion of the polymer segments and solvent molecules resulting in the shear stresses on the polymer chain leads to the scission of the polymer chain.[39] During the ultrasonic degradation, no chemical changes take place and only the most susceptible bonds break resulting in the polymer. As the superabsorbents AA/SA-1 and AA/SA/AM-1 have high equilibrium swelling capacities, that is, 306.80 and 621.69 g of water/g of SAP, respectively, their effective concentrations are 3.36 and 1.61 g L^{-1}, respectively. These effective concentrations fall in the same range as used for the ultrasonic degradation of polymer solutions by other authors.[40] Hence, the SAPs are also expected to undergo ultrasonic degradation by the same mechanism as that followed by linear polymers.

The ultrasonic degradation of the AA/SA-1 superabsorbent (0% AM content) at different ultrasound intensities was carried out in its equilibrium swollen state. The ultrasound intensities were determined by calorimetric method[41] and were found to be 0.670, 0.394, 0.164, 0.042, and 0.011 W cm^{-2} for the input voltage of 180, 170, 160, 150, and 100 V, respectively. Figure 12 shows the variation in the viscosity of the AA/SA-1 gels with ultrasonication time for different ultrasound intensities. The inset of Figure 12 shows the variation of ln Y with time at different intensities. Based on eq. (8), the slope of this plot gives $\kappa_{US}\mu_{lim}$, and the ultrasonic degradation rate coefficient (κ_{US}) are determined by dividing the slope by the limiting viscosity (μ_{lim}). The limiting viscosities were determined by running the degradation experiments until there was no more reduction in the viscosity of the gel. The ultrasonic degradation rate

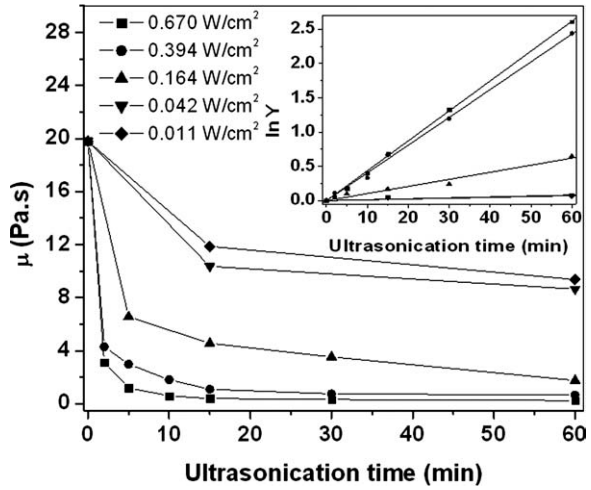

Figure 12 Variation in the viscosity of AA/SA-1 with ultrasonication time at different ultrasound intensities. The inset shows the time variation of ln *Y*.

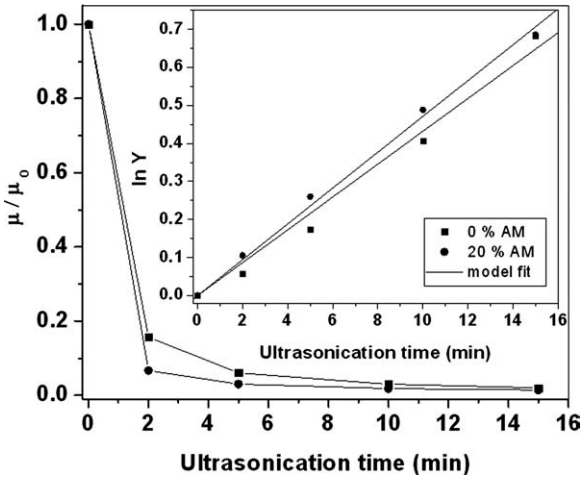

Figure 14 Change in the normalized viscosity of the AA/SA-1 and AA/SA/AM-1 SAPs with ultrasonication time. The inset shows the time variation of ln *Y*.

coefficients increase with the increasing ultrasound intensity as shown in Figure 13. The linear relationship between the limiting viscosity and the ultrasound intensity is also shown in Figure 13. A similar linear relationship between the limiting molecular weight and the ultrasound intensity has been found for the degradation of polystyrene in toluene.[42]

Figure 14 shows the reduction in normalized viscosity with ultrasonication time for AA/SA-1 and AA/SA/AM-1 superabsorbents. The inset figure shows the time variation of ln *Y*, and the ultrasonic degradation rate coefficients obtained from the slope are 0.21 and 0.43 Pa^{-1} s^{-2} for 0 and 20% AM content, respectively. AA/SA/AM-1 has higher equilibrium swelling capacity (621.7 g of water/g of SAP) than that of AA/SA-1 (306.8 g of water/g of SAP), and therefore, the concentration of AA/SA-1 is almost two times of that of the AA/SA/AM-1. The

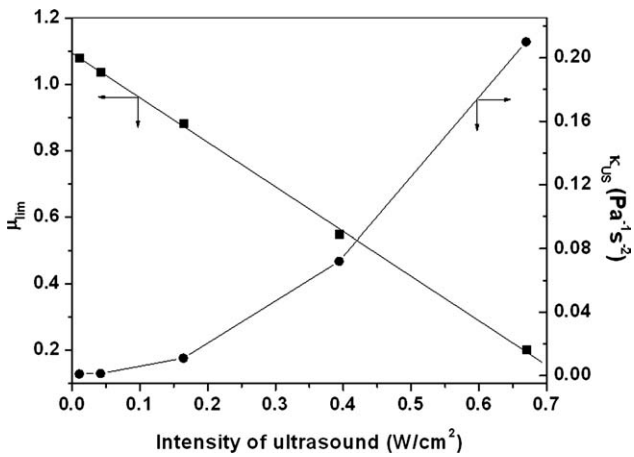

Figure 13 Variation of limiting viscosity of the SAP and the ultrasonic degradation rate coefficient with the intensity of the ultrasound.

viscosity increases with increasing concentration and the molecules become less mobile. The stress applied on polymer chain reduces as the velocity gradients diminish in the vicinity of the collapsing bubbles. Furthermore, at higher polymer concentrations, the solvent flow is disturbed by a larger number of polymer chains resulting in the diminished intensity of cavitation.[29,40] As a result, the ultrasonic degradation decreases with increasing concentration of the polymer solutions, and AA/SA-1 degrades at a lower rate than AA/SA/AM-1. These results are in conformity with those reported in the literature,[39,43] in which increased polymer concentration caused an increment in molecular coil overlap resulting in reduced rate of degradation due to reduced cavitation intensity.

The mechanism of degradation of SAPs by photo, thermal, and ultrasound are widely different. In photodegradation, the polymer bonds break due to absorption of high-energy UV radiation, whereas the thermal degradation of SAPs occurs due to the removal of volatiles and subsequent scission of polymer chains. During ultrasonic degradation, the polymer chains undergo scission because of the mechanical stresses resulting due to cavitation. Moreover, photodegradation and ultrasonic degradation were carried out in the equilibrium swollen stage of the SAPs, whereas thermal degradation was carried out in dry state. Thus, it is not possible to compare the results of photo, thermal, and ultrasonic degradation processes. However, we have shown that the SAPs can be degraded by various techniques and that the mechanisms of degradation are different in each technique.

CONCLUSIONS

Poly(acrylic acid-*co*-sodium acrylate-*co*-acrylamide) superabsorbents synthesized by inverse suspension

polymerization technique had a wide range of equilibrium swelling capacities and swelling rates. Copolymeric AA/SA/AM-1 had highest swelling capacity, and homopolymeric AM-1 had lowest swelling capacity. Homopolymeric AA/SA-1 superabsorbent had highest rate of swelling. The swelling of the SAPs followed the first order kinetics for which rate constants and equilibrium parameters were determined. The photodegradation and ultrasonic degradation of crosslinked three-dimensional networks resulted in linear water-soluble polymers. The photodegradation of all the SAPs, carried out in their equilibrium swollen state, took place in two stages based on the variation in swelling of the SAPs. However, the mechanism of degradation remained the same. The first stage was marked with increment in the swelling capacities because of the lowering of the crosslink density, and the second stage showed drastic decrease in the swelling capacity and residual weight of the SAP because of the rupture of the crosslinked network resulting in the formation of water-soluble polymers. The resistance to UV radiation increased with increasing AM content. TGA of the SAPs indicated reduction in the thermal stability of AA/SA-1 with the addition of AM. The ultrasonic degradation rate of the superabsorbents increased with increase in the intensity of the ultrasound. AA/SA/AM-1 (0% AM) had higher swelling capacity and lower ultrasonic degradation rate than AA/SA-1 (0% AM) with lower polymer concentration, and therefore, the former had a lower ultrasonic degradation rate than the latter. Thus, it is possible to obtain SAPs with desired equilibrium swelling capacity and resistance to UV radiation, ultrasound, and thermal degradation by copolymerizing AA/SA with AM.

The authors thank the department of science and technology, India, for financial support. The corresponding author thanks the department for the Swarnajayanthi fellowship.

References

1. Argade, A. B.; Peppas, N. A. J Appl Polym Sci 1998, 70, 817.
2. Lee, W. F.; Shieh, C. H. J Appl Polym Sci 1999, 73, 1955.
3. Takao, S.; Rei, U.; Haruyasu, T.; Kenji, U.; Akira, M. J Appl Polym Sci 2005, 98, 731.
4. Rodriguez, E.; Katime, I. J Appl Polym Sci 2003, 90, 530.
5. Abd El-Aal, S. E.; Hegazy, E. A.; AbuTaleb, M. F.; Dessouki, A. M. J Appl Polym Sci 2005, 96, 753.
6. Karadag, E.; Uzum, O. B.; Saraydin, D. Eur Polym J 2002, 38, 2133.
7. Yao, K. J.; Zhou, W. J. J Appl Polym Sci 1994, 53, 1533.
8. Zhou, W. J.; Yao, K. Y.; Kurth, M. J. J Appl Polym Sci 1996, 62, 911.
9. Mudiyansel, T.; Neckers, D. J. J Polym Sci Part A: Polym Chem 2008, 46, 1357.
10. Beltran, S.; Baker, J. P.; Hoope, H. H.; Blanch, H. W.; Prausnitz, J. M. Macromolecules 1991, 24, 549.
11. Yao, K. J.; Tang, Y. B. J Appl Polym Sci 1992, 45, 349.
12. Omidian, H.; Hashemi, S. A.; Sammes, P. G.; Meldrum, I. G. Polymer 1998, 39, 3459.
13. Liu, M.; Guo, T. J Appl Polym Sci 2001, 82, 1515.
14. Chen, X. P.; Shan, G. R.; Huang, J.; Huang, Z. M.; Weng, Z. X. J Appl Polym Sci 2004, 92, 619.
15. Yarimkaya, S.; Basan, H. J Macromol Sci Pure Appl Chem 2007, 44, 699.
16. Askari, F.; Nafisi, H.; Omidian, H.; Hashemi, S. A. J Appl Polym Sci 1993, 50, 1851.
17. Lu, S.; Duan, M.; Lin, S. J Appl Polym Sci 2003, 88, 1536.
18. Karadag, E.; Saraydin, D. Polym Bull 2002, 48, 299.
19. Zhang, J.; Sun, M. W.; Zhang, L.; Xie, X. M. J Appl Polym Sci 2003, 90, 1851.
20. Xue, W.; Champ, S.; Huglin, M. B. Polymer 2001, 42, 3665.
21. Esposito, F.; Del Nobile, M. A.; Mensitieri, C.; Nicolais, L. J Appl Polym Sci 1996, 60, 2403.
22. Uzum, O. B.; Kundakci, S.; Durukan, H. B.; Karadag, E. J Appl Polym Sci 2007, 105, 2646.
23. Zhang, J.; Wang, Q.; Wang, A. Carbohydr Polym 2007, 68, 367.
24. Liu, J.; Wang, Q.; Wang, A. Carbohydr Polym 2007, 70, 166.
25. Eid, M.; Abdel-Ghaffar, M. A.; Dessouki, A. M. Nucl Instrum Methods Phys Res Sect B 2009, 267, 91.
26. Tanuma, H.; Kiuchi, H.; Kai, W.; Yazawa, K.; Inoue, Y. J Appl Polym Chem 2009, 114, 1902.
27. Lanthong, P.; Nuisin, R.; Kiatkamjornwong, S. Carbohydr Polym 2006, 66, 229.
28. Li, X.; Cui, Y. J Appl Polym Sci 2008, 108, 3435.
29. Price, G. J.; Smith, P. F. Polym Int 1991, 24, 159.
30. Vijayalakshmi, S. P.; Madras, G. Polym Degrad Stab 2005, 90, 116.
31. Shukla, N. B.; Darabonia, N.; Madras, G. J Appl Polym Sci 2009, 112, 991.
32. Shukla, N. B.; Madras, G. Ind Eng Chem Res 2011, 50, 10918.
33. Flory, P. J. Principles of Polymer Chemistry; Cornell University Press: Ithaca, NY, 2006.
34. Pourjavadi, A.; Ghasemzadeh, H.; Mojahedi, F. J Appl Polym Sci 2009, 113, 3442.
35. Castel, A. D.; Ricard, A.; Audebert, R. J Appl Polym Sci 1990, 39, 11.
36. Omidian, H.; Hashemi, S. A.; Sammes, P. G.; Meldrum, I. Polymer 1998, 39, 6697.
37. Vinu, R.; Madras, G. J Phys Chem B 2008, 112, 8928.
38. Leung, W. M.; Axelson, D. E.; Van Dyke, J. D. J Polym Sci Part A: Polym Chem 1987, 25, 1825.
39. Price, G. J. In Advances in Sonochemistry; Mason, T. J., Ed.; JAI Press: Cambridge, UK, 1990; Vol. 1, p 231.
40. Price, G. J.; Smith, P. F. Eur Polym J 1993, 29, 419.
41. Kotronarou, A.; Mills, G.; Hoffmann, M. R. Environ Sci Technol 1992, 26, 2420.
42. Price, G. J.; Smith, P. F. Polymer 1993, 34, 4111.
43. Nguyen, T. Q.; Liang, Q. J.; Kausch, H. H. Polymer 1997, 38, 3783.